U. S. N. A. --- Trident Scholar project report; no. 344 (2006)

Using All-optical Wavelength Conversion for Routing in Optical Local Area Networks

by

Midshipman 1/c Clifford N. Jessop, Class of 2006
United States Naval Academy
Annapolis, Maryland

Certification of Advisors Approval

Associate Professor R. Brian Jenkins
Electrical Engineering Department

_____
(signature)

_____
(date)

CAPT Robert Voigt, USN
Electrical Engineering Department

_____
(signature)

_____
(date)

Acceptance for the Trident Scholar Committee

Professor Joyce E. Shade
Deputy Director of Research & Scholarship

_____
(signature)

_____
(date)

USNA-1531-2

REPORT DOCUMENTATION PAGE

Form Approved
OMB No. 074-0188

1. AGENCY USE ONLY (Leave blank)	2. REPORT DATE	3. REPORT TYPE AND DATE COVERED
	8 May 2006	

4. TITLE AND SUBTITLE
Using all-optical wavelength conversion for routing in optical local area networks

5. FUNDING NUMBERS

6. AUTHOR(S)
Jessop, Clifford N. (Clifford Nicholas), 1983-

7. PERFORMING ORGANIZATION NAME(S) AND ADDRESS(ES)		8. PERFORMING ORGANIZATION REPORT NUMBER

9. SPONSORING/MONITORING AGENCY NAME(S) AND ADDRESS(ES)		10. SPONSORING/MONITORING AGENCY REPORT NUMBER
US Naval Academy Annapolis, MD 21402		**Trident Scholar project report no. 344 (2006)**

11. SUPPLEMENTARY NOTES

12a. DISTRIBUTION/AVAILABILITY STATEMENT	12b. DISTRIBUTION CODE
This document has been approved for public release; its distribution is UNLIMITED.	

13. ABSTRACT All-optical wavelength conversion is a process that is used to reduce the number of optical-electrical-optical (O-E-O) conversions in an optical network. Limiting O-E-O conversions reduces latency for signals propagating through the network. The focus of this project is to implement all-optical wavelength conversion in the physical layer of an optical local area network (LAN) to observe its effect on system performance. Several types of wavelength converters have been considered for such a network, specifically those using cross-gain modulation (XGM), cross-phase modulation (XPM), four wave mixing (FWM), and difference frequency generation (DFG). Particular attention is paid to the effect on latency, bit error rate (BER), and analog spur free dynamic range (SFDR). Analyses have been done using both computer simulation and a hardware test bed, emphasizing XGM and XPM converters. Ultimately, all-optical wavelength converters are desired for use in mixed signal networks, where both analog and digital data propagate through the network. As a baseline, measurements taken on a particular wavelength division multiplexed LAN indicate the capacity to handle 10 Gbps digital signals and analog operation with a spur free dynamic range (SFDR) of 113 dB-Hz2/3 before wavelength conversion. This project examines the effect of wavelength conversion in a mixed signal environment with an emphasis on reducing network latency without significantly compromising network performance as measured by BER and SFDR.

14. SUBJECT TERMS All-Optical Wavelength Conversion ; XGM ; LAN	15. NUMBER OF PAGES **46**
	16. PRICE CODE

17. SECURITY CLASSIFICATION OF REPORT	18. SECURITY CLASSIFICATION OF THIS PAGE	19. SECURITY CLASSIFICATION OF ABSTRACT	20. LIMITATION OF ABSTRACT

Abstract

All-optical wavelength conversion is a process that is used to reduce the number of optical-electrical-optical (O-E-O) conversions in an optical network. Limiting O-E-O conversions reduces latency for signals propagating through the network. The focus of this project is to implement all-optical wavelength conversion in the physical layer of an optical local area network (LAN) to observe its effect on system performance. Several types of wavelength converters have been considered for such a network, specifically those using cross-gain modulation (XGM), cross-phase modulation (XPM), four wave mixing (FWM), and difference frequency generation (DFG). Particular attention is paid to the effect on latency, bit error rate (BER), and analog spur free dynamic range (SFDR). Analyses have been done using both computer simulation and a hardware test bed, emphasizing XGM and XPM converters. Ultimately, all-optical wavelength converters are desired for use in mixed signal networks, where both analog and digital data propagate through the network. As a baseline, measurements taken on a particular wavelength division multiplexed LAN indicate the capacity to handle 10 Gbps digital signals and analog operation with a spur free dynamic range (SFDR) of 113 dB-$Hz^{2/3}$ before wavelength conversion. This project examines the effect of wavelength conversion in a mixed signal environment with an emphasis on reducing network latency without significantly compromising network performance as measured by BER and SFDR.

Keywords: All-Optical Wavelength Conversion, XGM, LAN

Acknowledgements

Associate Professor R. Brian Jenkins, Electrical Engineering Department and **CAPT Robert Voigt**, Electrical Engineering Department Chair, for all the work they put in as my advisors. This project never would have been possible without their guidance and support.

Bonnie Jarrell, Electrical Engineering Department Secretary, for all her help throughout the year.

Professor Joyce Shade, Deputy Director of Research & Scholarship for the opportunity and the support to make this project a reality.

Table of Contents

Table of Figures

Introduction

Computer networks are a vital part of our society. We live in an increasingly interconnected world where the ability to communicate and share data quickly and efficiently is a necessary part of daily life. As the processing speeds of modern computers increase, the need for higher speed networks continues to grow. Whether it is the Internet, a local area network (LAN), or a metropolitan size network, larger bandwidth and faster data transfer rates are demanded from every part of society: public, private, and the military.

Fiber optic communication provides a solution to the increased demand for bandwidth and throughput. The bandwidth of optical fibers is large, and there is very little attenuation or degradation over long distances. This bandwidth can be used even more efficiently through the use of dense wavelength division multiplexing (DWDM), in which multiple streams of data can be sent over the same optical cable at the same time by using a different wavelength of light for each data stream. Also, losses that occur can now be easily compensated by using optical amplifiers instead of expensive electrical regenerators.

Optical cable also supports the simultaneous transmission of both analog and digital data streams over the same fiber. This transparency to mixed signals is very attractive to network designers both in and out of the military. For the Navy it means that an entire ship's network could be implemented using optical fiber with analog sensor information and digital fire control information passing over the same cable. This saves both money and installation time while the bandwidth provided by the optical fiber supports increased network performance. In the public sector, mixed signal optical networks could be used to deliver television, voice, and Internet connections into a household on a single line.

Currently, optical cable is used mainly as the backbone of large networks, sometimes referred to as wide area networks, mostly because of its high bandwidth and the low loss. As networks are scaled to smaller sizes, such as metropolitan sized networks and local area networks (LAN), the use of optical cable as a transmission medium is increasing, but less common. The electronics used to route data at this network level are far slower in terms of bandwidth than their optical counterparts. This leads to a bottleneck commonly referred to as the "metro-gap" which prevents the end users of the data from taking full advantage of the optical throughput capabilities of the network backbone. [1] One way to reduce the "metro-gap" would be to extend the transition from the optical to the electronic domain further down into the LAN or to the end network node itself. In order to do this however an all-optical routing system is needed. Wavelength conversion is a new technology that may provide this capability.

Background

In many network topologies, data is fragmented into packets with each packet routed from a source node to a destination node by making a number of "hops" through other nodes. End nodes are usually defined as computers, and intermediate nodes are often routers or gateways into another network. Each packet contains the necessary addressing information to insure proper delivery. In optical packet switching networks, packets must be converted from an optical format into an electronic format at intermediate nodes in order to make a routing decision. The router then forwards the packet on the appropriate outgoing interface. The packet must be converted back into an optical signal in order to be transmitted on the optical fiber to go to the next node in the network. This optical-electrical-optical (O-E-O) interface at intermediate nodes introduces latency because the delay through the electronic circuitry in the node is slow relative to the propagation delay of the packets on the optical fiber.

All-optical wavelength conversion offers a possible solution to the bottleneck problem by reducing the number of O-E-O conversions that need to be made as data is routed through a network. This decreases latency since the relatively slow electronics are removed from the network path and data can stay in an optical format throughout the routing process.

As an example, consider the eight node ShuffleNet constructed by Adam Fisher as part of his Trident project in 2004, as seen in Figure 1. This is a regular network with a mesh topology. Each node is connected to two other nodes at its inputs and two nodes at its outputs. This sets a maximum of three hops between any two nodes in an eight node ShuffleNet. The nodes on the left are repeated on the right to simplify the interconnection diagram. Figure 1 shows one route between Node 0 and Node 5 that requires three hops (Node 0 to Node 7, Node 7 to Node 4, Node 4 to Node 5).

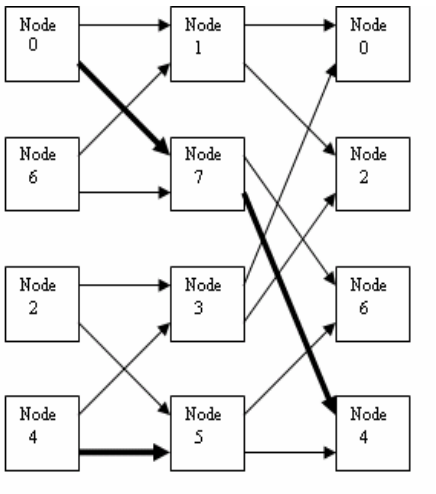

Figure 1: Spatial representation of an eight node network.

While the network in Figure 1 could be connected using 16 optical fibers, an alternate representation of the ShuffleNet topology can be seen in Figure 2. In this figure each different color corresponds to a different frequency of light traveling through a single fiber ring. The

symbols Tx and Rx indicate the positions of transmitters and receivers, respectively. As this figure shows, some signals bypass certain nodes and go straight through the add/drop multiplexers (ADM) which are used to add or remove certain frequencies from the fiber. A careful analysis of Figure 2 shows that the connections between the nodes are identical to those in Figure 1. However, O-E-O conversions are still required in each node to make routing decisions between a receiver and transmitter. With wavelength conversion however, latency at each node can be reduced by using a wavelength converter to perform the required routing function.

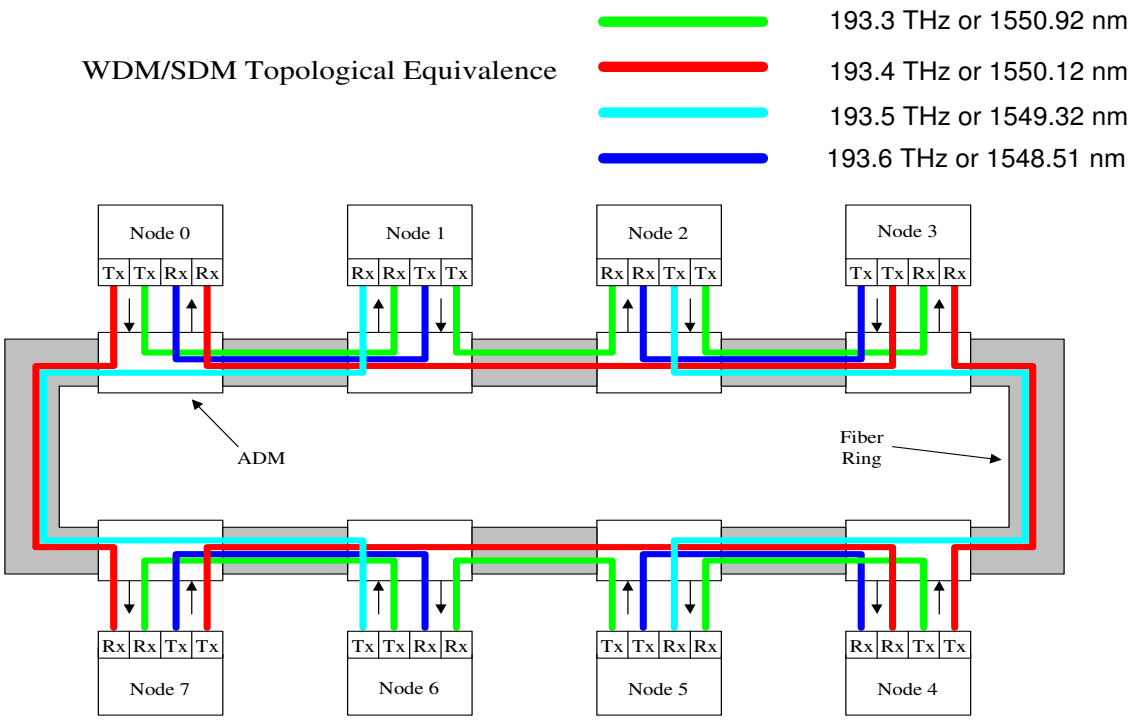

Figure 2: Eight-node ShuffleNet implemented with four wavelengths and one fiber ring. [2]

There are four basic techniques that have been investigated for performing wavelength conversion: cross gain modulation (XGM), cross phase modulation (XPM), four wave mixing (FWM), and difference frequency generation (DFG). Each method has advantages and

disadvantages. XGM is perhaps the easiest wavelength conversion scheme to implement. This technique uses a semiconductor optical amplifier (SOA) to convert amplitude-modulated data from one wavelength to another. It works by using the gain saturation characteristics of the SOA to imprint the amplitude modulation of the incoming signal onto a continuous wave (CW) signal on a different wavelength. Wavelength converters using XGM have many benefits over the current opto-electronic method, such as a possible bit rate of greater than 10 Gbps and low electrical power consumption. However, XGM wavelength conversion can result in a signal with a low extinction ratio, defined as the ratio of the power of a logical high signal to the power of a logical low signal. This results in an increased bit error rate (BER), where BER is defined as the ratio of bits received in error to the total number of bits transmitted. The XGM conversion process also causes a large chirp, a condition where the instantaneous frequency varies across the pulse, as seen in Fig. 3. In this example, lower frequencies move to the front of the pulse while higher frequencies move to the rear. This chirp worsens the impact of dispersion in the optical fiber over longer lengths typical of wide area networks. Both of these effects limit cascadability, the ability to place wavelength converters back-to-back throughout the network. XGM wavelength converters are also typically used only with digital data. They are not transparent to data type and thus probably cannot be used in a mixed signal environment. [3] This is verified as part of the project.

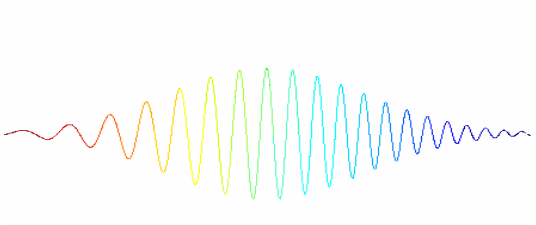

Figure 3: Pulse Chirp: Lower frequencies in the front, higher frequencies in the rear

Wavelength conversion can also be realized by using XPM. With XPM the amplitude modulated input signal causes a modulation in the phase of a CW signal, usually through the use of an SOA. Interferometric techniques can then be used at the output of the SOA to convert the phase-modulated signal to an amplitude-modulated signal on the new wavelength. While the XPM conversion technique is also not transparent to mixed signals, it has a better signal-to-noise ratio (SNR) than the XGM technique. [4]

The third technique for wavelength conversion is FWM. This technique combines an input data signal (at frequency f_{signal}) with a much stronger pump signal (at frequency f_{pump}) in a nonlinear fiber or an SOA. The beat signals caused by mixing these waves produces two new waves with frequencies of $(2f_{pump} - f_{signal})$ and $(2f_{signal} - f_{pump})$ that are called the mixing signal and the satellite signal, respectively, as shown in Figure 4. The mixing signal becomes the output signal of the process and the other three frequencies can be filtered out by an optical band pass filter. One important benefit of four-wave mixing is that the amplitude and phase of the output wave are linear combinations of the input and pump signals. Therefore FWM offers strict data format transparency, which enables FWM converters to handle mixed analog and digital data signals. Unfortunately, the SNR for FWM converters tends to be quite low, so cascadability is currently limited. [5]

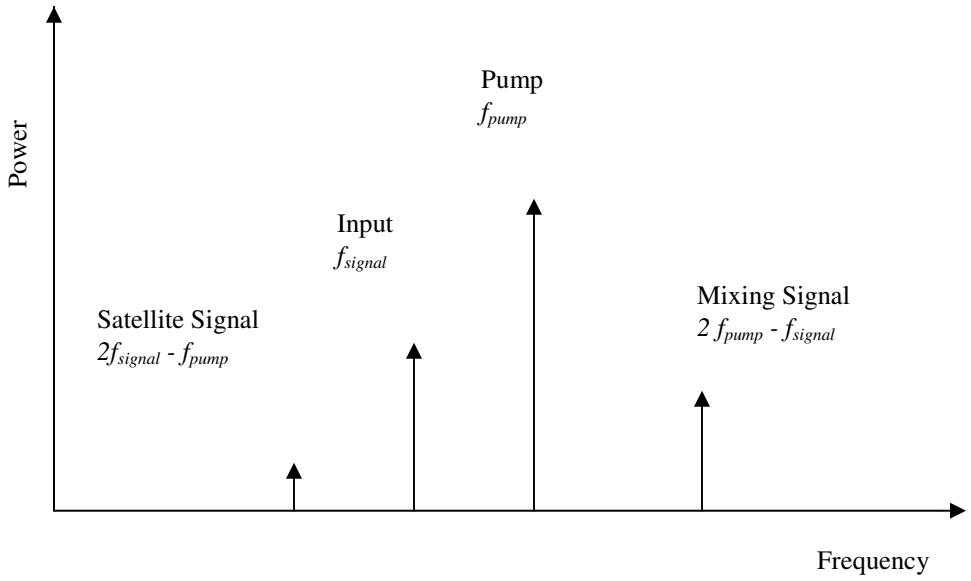

Figure 4: Spectrum of frequencies created by four-wave mixing. [5]

The last of the wavelength conversion techniques is difference frequency generation (DFG). This is similar to four-wave mixing in that both techniques mix two input signals, an input signal carrying data and a CW pump signal. DFG, however, does not produce the extra satellite wave that four-wave mixing gives us. DFG has many benefits over the other three conversion techniques and would likely be the best technique for mixed signal formats. However, DFG is more expensive because of the strict manufacturing standards needed during the fabrication of periodically poled Lithium-Niobate devices used in such converters. Further advantages and disadvantages of the four techniques are summarized in Table 1.

Wavelength Conversion Technique	Advantages	Disadvantages
Cross Gain Modulation (XGM)	• Bite rate > 10 Gbps • Large dynamic range • Easiest to implement	• Low extinction ratio • Chirp • Limited data format transparency
Cross Phase Modulation (XPM)	• Bit rate > 40 Gbps • High SNR	• Limited data format transparency • Narrow dynamic range • Can be sensitive to the polarization of incoming light
Four Wave Mixing (FWM)	• Strict data format transparency • Low and reversible chirp • Bit rate > 10 Gbps	• Low SNR which limits cascadability • Small range of wavelengths that can be converted
Difference Frequency Generation (DFG)	• Bit rate > 10 Gbps • Can simultaneously convert multiple wavelengths • Large input bandwidth • Strict data format transparency • Good SNR	• Expensive due to strict tolerances needed during fabrication

Table 1: Advantages and disadvantages of different wavelength conversion topologies [5]

Project Overview

In this project an all-optical wavelength converter has been simulated, built, and integrated into a LAN. The research focuses primarily on XGM wavelength converters because of the simple topology and and promising early simulation results. Simulations were also done on XPM converter topologies, although none were constructed in hardware. Since XGM converters rely on SOAs for conversion, an overview of SOA operation is presented, along with simulation and hardware results for the converter.

SOA Mathematical Analysis

A thorough knowledge of the SOA gain dynamics is critical to understanding how an XGM converter operates. A brief mathematical explanation, which largely follows that presented in [6], of the gain dynamics in an SOA is presented below. These equations describe the gain dynamics in an SOA when a pulse of light is incident on the device and the recovery period after the pulse has passed.

The gain, and hence the output power, of an SOA is a function of the carrier density, *N*, the number of electrons in an elevated energy level per unit volume of the SOA. Therefore, our analysis of the SOA gain dynamics begins with the differential equation that describes the carrier density as a function of time *t* and position *z* within the SOA:

$$\frac{\partial N(z,t)}{\partial t} = \frac{I}{eV} - \frac{N(z,t)}{\tau} - \frac{P(z,t)\Gamma g[N(z,t) - N_T]}{h\nu A}. \quad (1)$$

In this equation I is the drive current of the SOA; e is the charge of an electron; V is the volume of the SOA's active region; τ is the carrier lifetime that describes how quickly excited electrons drop back to their normal energy levels; $P(z,t)$ is the optical power in the SOA; Γ is a mode confinement factor, a measure of how well the optical power is confined to the active region of the SOA; g is a gain coefficient; N_T is the transparency carrier density (the carrier density at which we have unity gain, such that the power level out of the device is equal to the power level into the device); $h\nu$ is the energy of an incoming photon, and A is the cross sectional area of the SOA active region.

Given that eV is a constant, the first term on the right hand side of Equation (1) describes an increase in carrier density as more electrons are pumped to a higher energy level by the SOA drive current. The second term on the right side of the equation describes a decrease in carrier

density as electrons fall back to their original energy levels, a process known as recombination. This process may or may not release light, and the light that is released can have a range of optical frequencies and phases, a process known as spontaneous emission. This leads to the introduction of noise into the system. Finally, the last term on the right describes a process known as stimulated emission, whereby an incoming photon triggers a recombination that releases another photon that is identical in frequency and phase to the original incoming photon. This is the process by which gain is produced in an SOA. Therefore, Equation (1) can be expressed in words this way: the rate of change of carrier density inside the SOA with respect to time is dependent on the amount of electrons pumped to a higher energy level by the drive current, the amount of electrons that spontaneously recombine, and the amount of electrons that recombine due to stimulated emission. This process is illustrated by Figure 5. Here, the electrons that have been pumped to a higher energy level (E_{upper}) are represented by the dashed lines at the top of the figure. The incoming photon of light, triggers the recombination of one of these electrons and results in the release of an additional photon of light.

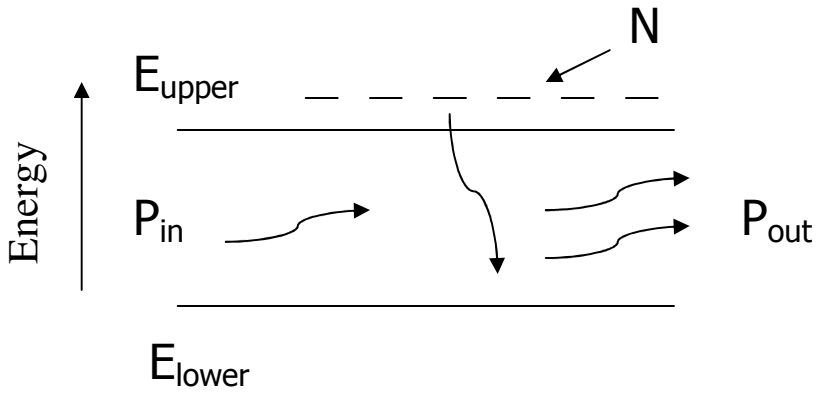

Figure 5: Stimulated emission in an SOA

The optical power in the SOA is described by the following differential equation, describing the rate of change of optical power with respect to position:

$$\frac{\partial P(z,t)}{\partial z} = P(z,t)\Gamma g[N(z,t) - N_T] - P(z,t)\alpha_D . \quad (2)$$

The first term on the right hand side of the equation describes the increase in optical power due to stimulated emission and the second term describes the decrease in optical power due to loss in the waveguide, as determined by the attenuation coefficient α_D in m^{-1}. Assuming that the carrier density is independent of z and P for very small input powers allows us to solve this differential equation by separation of variables over the length L of the SOA. This yields an expression for the SOA steady state gain, G_0, at time t_{ss}, where N_S is the steady state carrier density:

$$G_0 = \frac{P_{out}}{P_{in}} = e^{[\Gamma g L (N_S - N_T) - L\alpha_D]}, \quad (3)$$

where $P_{out} = P(L,t_{ss})$ and $P_{in} = P(0,t_{ss})$.

If we treat the SOA as a short device then we can approximate the total number of carriers per cross sectional area of the SOA by integrating over the length of the SOA:

$$N_{tot}(t) = \int_0^L (N(z,t) - N_T)dz . \quad (4)$$

Using Equation (4) we can represent the gain of the SOA as a function of time by integrating Equation (2) over the length of the SOA, as in:

$$\int_{P_{in}}^{P_{out}} \frac{\partial P(z,t)}{P(z,t)} = \Gamma g N_{tot}(t) - \alpha_D L . \quad (5)$$

Hence, the small signal gain $G(t)$ is given by

$$G(t) = \frac{P(L,t)}{P(0,t)} = e^{[\Gamma g N_{tot}(t) - \alpha_D L)} . \quad (6)$$

When a pulse of optical energy is incident on the SOA, the gain dynamics become complicated because the incoming pulse quickly depletes carriers in the SOA, pushing the device

into saturation. For saturation by a short pulse, we begin by neglecting the first two terms on the right side of Equation (1), assuming these are negligible over the duration of the pulse compared with the spontaneous emission process. Upon integration over the length *L* of the SOA, Equation (1) becomes:

$$\frac{d}{dt}\int_0^L N(z,t)dz = \frac{d}{dt}N_{tot}(t) = \frac{-1}{h\nu A}\int_0^L P(z,t)\Gamma g[N(z,t) - N_T]dz, \tag{7}$$

where $\frac{dN_T}{dt} = 0$ since N_T is constant. If we solve Equation (2) for *P(z,t)* and we integrate both sides over the length of the SOA, we obtain the following approximation,

$$\int_0^L P(z,t)dz \approx \frac{L}{\ln(G_0)}[P_{out} - P_{in}], \tag{8}$$

where the relation given in Equation (3) is used to simplify the expression. Using Equation (2) we can rearrange the terms of Equation (7) to give

$$\frac{d}{dt}N_{tot}(t) = \frac{-1}{h\nu A}\int_0^L \left[\frac{\partial P(z,t)}{\partial z} + \alpha_D P(z,t)\right]dz\ . \tag{9}$$

Solving Equation (9) using the approximation in Equation (8) yields the rate of change of $N_{tot}(t)$ with respect to time,

$$\frac{dN_{tot}(t)}{dt} = -\frac{1+\frac{\alpha_D L}{\ln(G_0)}}{h\nu A}[P_{out}(t) - P_{in}(t)]. \tag{10}$$

If we solve Equation (6) for $N_{tot}(t)$ and differentiate with respect to time we obtain the following, where $G'(t) = dG(t)/dt$:

$$\frac{dN_{tot}(t)}{dt} = \frac{1}{\Gamma g}\left[\frac{G'(t)}{G(t)}\right]. \tag{11}$$

Combining Equations (10) and (11) and substituting $P_{out}(t)/P_{in}(t)$ with $G(t)$ yields

$$\frac{1}{\Gamma g}\left[\frac{G'(t)}{G(t)}\right] = \frac{-P_{in}(t)}{h\nu A}\left(1+\frac{\alpha_D L}{\ln(G_0)}\right)[G(t)-1]. \tag{12}$$

By grouping the terms in $G(t)$ and integrating both sides with respect to time, we arrive at the following equation:

$$\ln\left(\frac{1-\frac{1}{G_0}}{1-\frac{1}{G(t)}}\right) = \frac{\Gamma g\left(1+\frac{\alpha_D L}{\ln(G_0)}\right)}{h\nu A}\int_0^t P_{in}(t')dt', \tag{13}$$

where we have assumed that $G_0 = G(t=0)$. Since the energy injected by the pulse is

$$U_{in}(t) = \int_0^t P_{in}(t')dt', \tag{14}$$

and if we define the saturation energy of the SOA as

$$U_{sat} = \frac{h\nu A}{\Gamma g\left(1+\frac{\alpha_D L}{\ln(G_0)}\right)}, \tag{15}$$

we can express the gain of the SOA during the pulse transition as:

$$G(t) = \frac{1}{1-\left(1-\frac{1}{G_0}\right)e^{\left(\frac{-U_{in}(t)}{U_{sat}}\right)}}. \tag{16}$$

After the pulse exits the SOA, the carrier density and gain begin to recover. If we neglect the last term of Equation (1), assuming no incident optical power, we can use Equation (4) to derive the following differential equation which governs the replenishment of carriers from saturation:

$$\frac{dN_{tot}(t)}{dt} = \left(\frac{I}{eV}-\frac{N_T}{\tau}\right)L - \frac{N_{tot}(t)}{\tau}. \tag{17}$$

Equation (17) describes the transient and steady state response for $N_{tot}(t)$ during gain recovery, where the term in the parenthesis is the driving function. The initial condition and steady state value of N_{tot} can be determined using Equation (6), such that

$$N_{tot}(t_s) = \frac{\ln[G(t_s)] + \alpha_D L}{\Gamma g} \quad \text{(initial condition)}, \tag{18a}$$

$$N_{tot,ss} = \frac{\ln(G_0) + \alpha_D L}{\Gamma g} \quad \text{(steady state)}, \tag{18b}$$

where $t = t_s$ at the end of the input pulse. Using these boundary conditions and solving for $N_{tot}(t)$ from Equation (17) leads to the following equation describing the gain during recovery:

$$G(t) = G_0 \left(\frac{G(t_s)}{G_0} \right)^{e^{-(t-t_s)/\tau}} . \tag{19}$$

This analysis is most easily illustrated using Figure 6 which shows the change in gain with respect to time as an optical pulse transits an SOA. Initially, the gain of the device is G_0, represented by Equation (3). As the pulse propagates through the device, the gain drops as defined by Equation (16). Finally, after the pulse has passed through the device, the gain recovers as defined by Equation (19). These equations will later be the limiting factor in determining the performance constraints of an XGM converter. Because the gain takes so long to recover compared to its saturation time, at higher bit rates it is possible to have a subsequent pulse arrive at the SOA before its gain has had a chance to recover. This significantly degrades the output bit pattern and makes it much more difficult for a receiver to differentiate between what is supposed to be a logical high or low signal.

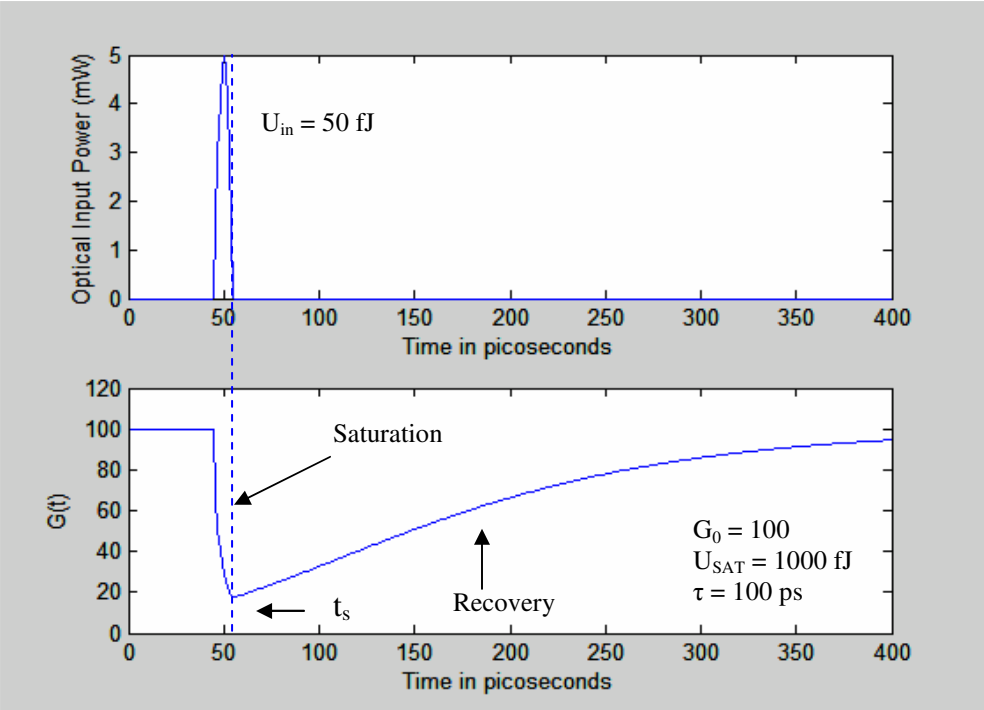

Figure 6: Gain dynamics of an SOA with an optical input pulse.

Simulation Results for Different Converter Configurations

VPI Photonics computer software was used to simulate different types of wavelength converters for this project. There were three main wavelength converter topologies that were simulated on VPI: XGM, XPM in a Mach-Zender Interferometer (MZI) configuration, and XPM in a Sagnac interferometer configuration.

Initial simulations focused on the simplest wavelength converter, specifically the XGM topology involving a single SOA. In this configuration a data signal on one wavelength (λ_1) in the 1550 nm band is multiplexed with light from a weaker, continuous wave (CW) laser at a different wavelength (λ_2), also in the 1550 nm region. The signals are then coupled to an SOA that is driven by an electrical current, *I*, that is typically between 300 and 800 mA. At the output of the SOA the signal on wavelength λ_2 is recovered using an optical bandpass filter with its

passband centered at λ_2. A block diagram of an XGM converter and the corresponding VPI schematic are shown in Figures 7 and 8, respectively.

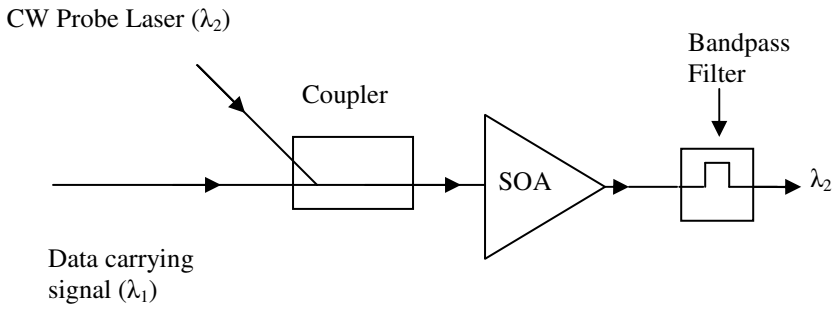

Figure 7: Block diagram of an XGM converter.

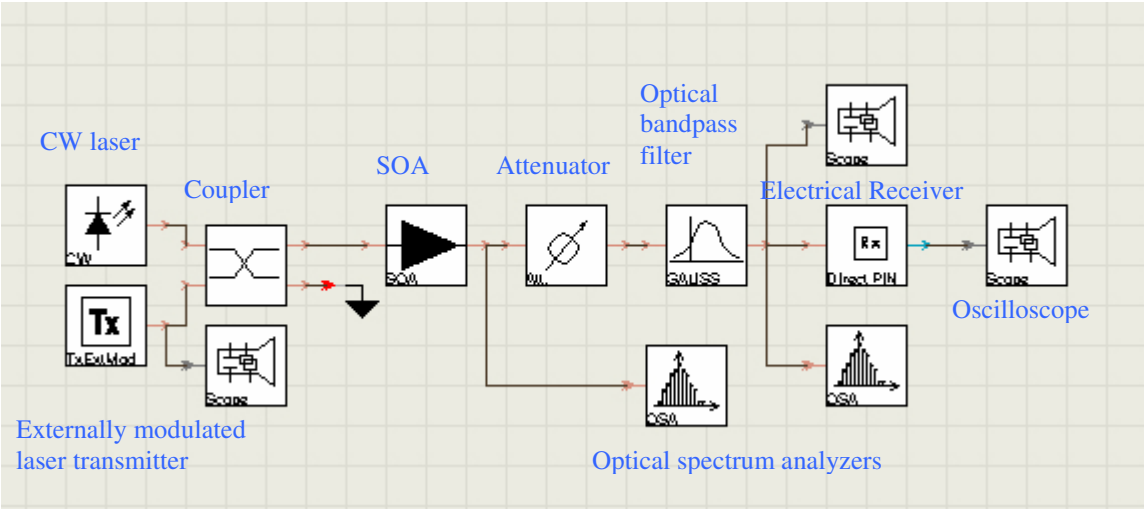

Figure 8: Schematic of an XGM converter in VPI Photonics.

The XGM converter operates according to the gain-saturation characteristic of an SOA shown in Figure 9. This graph shows that the gain falls off as the input power of the signal increases. Therefore, modulation of the input power caused by the data on one wavelength (λ_1) will cause variations in the gain of the SOA, and thus the power of the output wavelength (λ_2) will vary as well. When the incoming digital data on wavelength λ_1 is a logical high, the total input power to the SOA is higher and thus the gain of the SOA is lower, approaching 0 dB, or

unity gain. This means that the output power is roughly equal to the power input. Conversely, when the incoming data is a logical low, a lower input power is incident on the SOA and the gain is higher. For example, an input power of -30 dBm (or 1 μW) in Figure 9(a) results in a gain of approximately 30 dB, meaning that the output power will be about 1000 times greater than the input power. This variation in the gain of the SOA, due to the data transitions on λ_1, modulates the power level of the CW wave on λ_2, inverting the data from λ_1 and imprinting it onto λ_2, as shown in Figure 9(b).

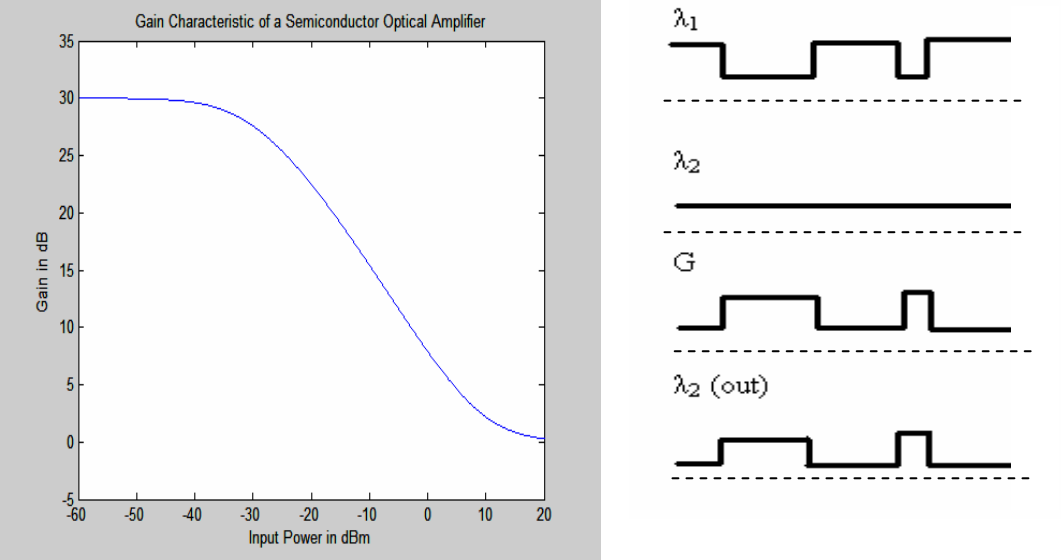

(a) Gain saturation curve **(b) Effect of data on gain and converter output**

Figure 9: Gain saturation characteristics of an SOA [7]

The periods in time where the gain drops in Figure 9(b) correspond to the saturation region of Figure 5. As more carriers recombine due to stimulated emission from an input pulse, there are fewer carriers available to provide gain. Thus, the gain drops as seen in Figure 6. Conversely, the periods where the gain rises correspond to the recovery region of Figure 6. The process shown in Figure 9(b) is idealized. In reality, the gain does not saturate or recover

instantaneously, and therefore the output of the XGM converter is really not sharp crisp rectangular pulses as seen in Figure 9(b).

Based on the XGM simulations, we were able to determine a general range of input powers and drive currents that would be needed to make the device work. We also quickly realized that it would be necessary to attenuate the output of the SOA to ensure the safety of the test equipment in the lab. Simulations also demonstrated that the maximum bit rate of the converter was directly related to the carrier lifetime (τ) that was discussed above. For small values of τ, the carriers recombine too quickly to allow modulation of the gain characteristic of the SOA. On the other hand with longer carrier lifetimes at high bit rates, subsequent pulses arrive at the SOA before the gain has had a chance to recover. This leads to a rapid degradation of the output bit stream as seen in the Figures 10 and 11 below. In Figure 11, the gain has not had a chance to fully recover before subsequent pulses arrive, which degrades the output bit stream. Simulations also showed that longer SOA lengths allowed higher bit rates through the device, though long SOAs are more difficult to manufacture. Finally, the extinction ratio of the output is degraded which increases the bit error rate. As an example, for the 10 Gbps stream in Figure 10 the extinction ratio is approximately 30 dB on the input data, whereas the output extinction ratio is approximately $\frac{300}{30} = 10$ (which is the same as 10 dB). While an extinction ratio of 10 dB may be sufficient over the relatively short distances required in a LAN, cascading converters leads to further degradation. This is a common disadvantage for XGM converters (see Table 1).

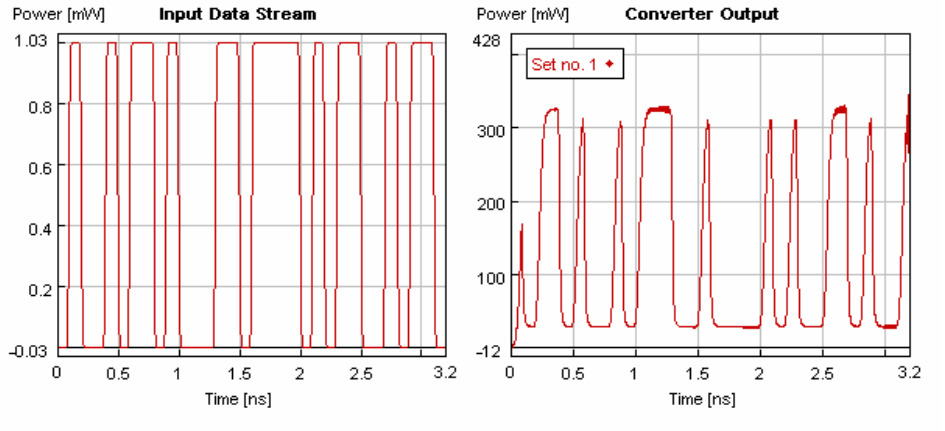

(a) 10 Gbps Input **(b) 10 Gbps Output**

Figure 10: XGM converter at 10 Gbps.

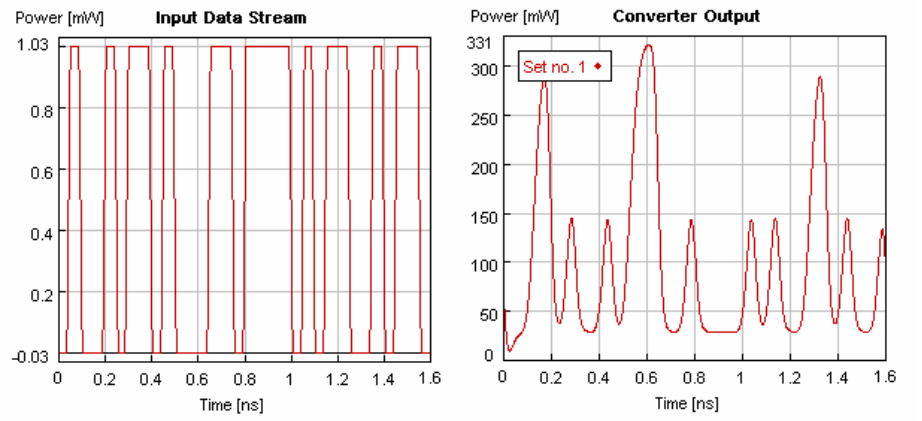

(a) 20 Gbps Input **(b) 20 Gbps Output**

Figure 11: XGM converter at 20 Gbps

One way to improve the converter's performance is to use both the phase and gain dynamics of the SOA to imprint data from one wavelength to another. This is the basis for XPM type converters. Two types of XPM converters were simulated: 1) a Mach-Zender interferometer (MZI) configuration, and 2) a Sagnac loop interferometer. Both use phase shifts caused by the SOAs to enhance either constructive or destructive interference at the output of the interferometer, thereby generating a well-defined output bit pattern.

In an XPM MZI configuration, CW light enters both arms of an MZI, as shown in Figure 12. A data signal on a different wavelength is also coupled into one of the arms of the interferometer and an SOA is placed in each arm. Each SOA impacts both the gain and phase of the CW light at λ_2. However, SOA 1 also modulates the gain and phase of the CW light in the upper arm according to the data pattern on λ_1. This process essentially imprints an inverted copy of the incoming data pattern onto the new wavelength. The original data signal is then removed by an optical bandpass filter. The simulation schematic for this configuration is shown in Figure 13.

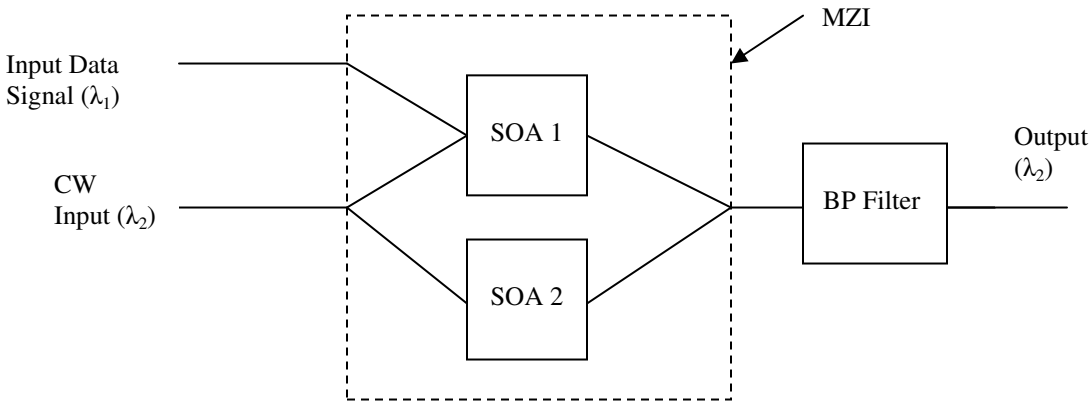

Figure 12: Diagram of an XPM MZI wavelength Converter.

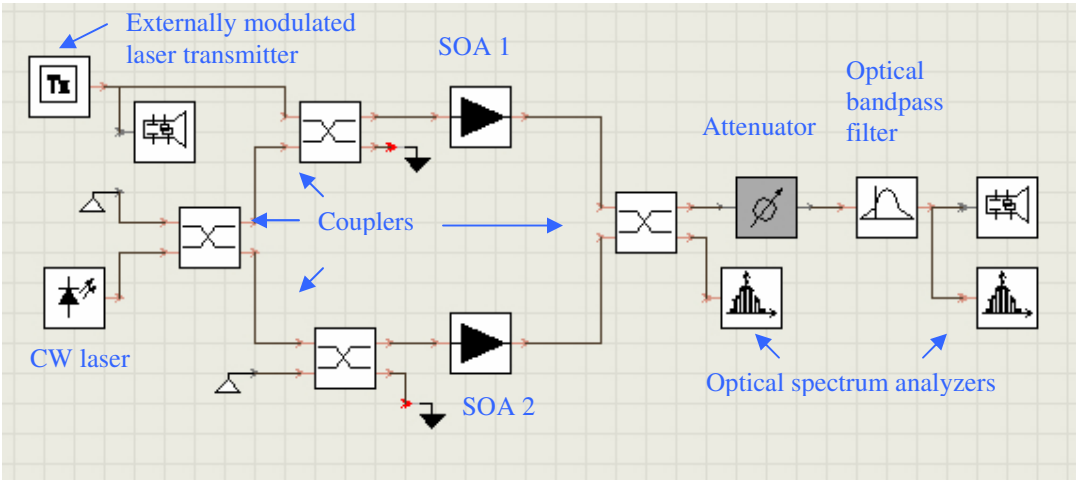

Figure 13: Schematic of an XPM MZI converter in VPI.

With this topology, simulated performance was much better at higher bit rates than with an XGM converter, as seen in Figure 14. Note that the extinction ratio is degraded much less with this configuration. However, actually constructing an XPM MZI converter may be more complicated than assembling an XGM converter. An XPM converter requires more precise phase control so the design constraints are sensitive to the input power levels, the SOA drive currents, the SOA characteristics, and the optical path length.

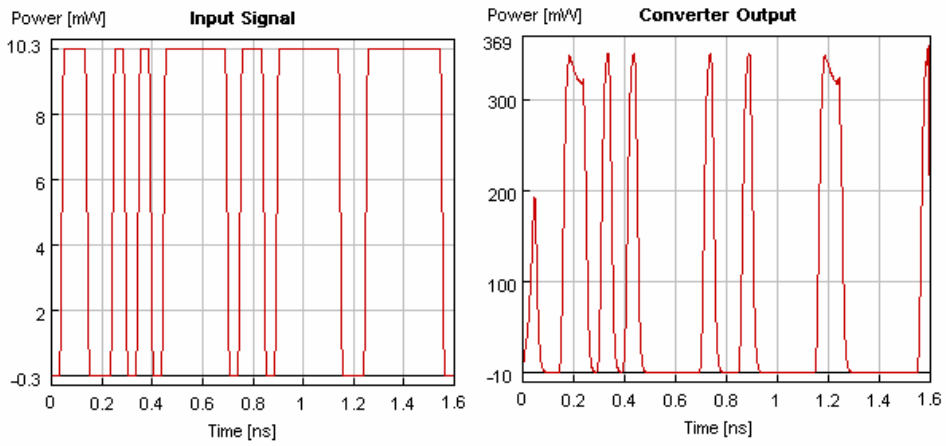

(a) 20 Gbps Input **(b) 20 Gbps Output**

Figure 14: XPM MZI at 20 Gbps.

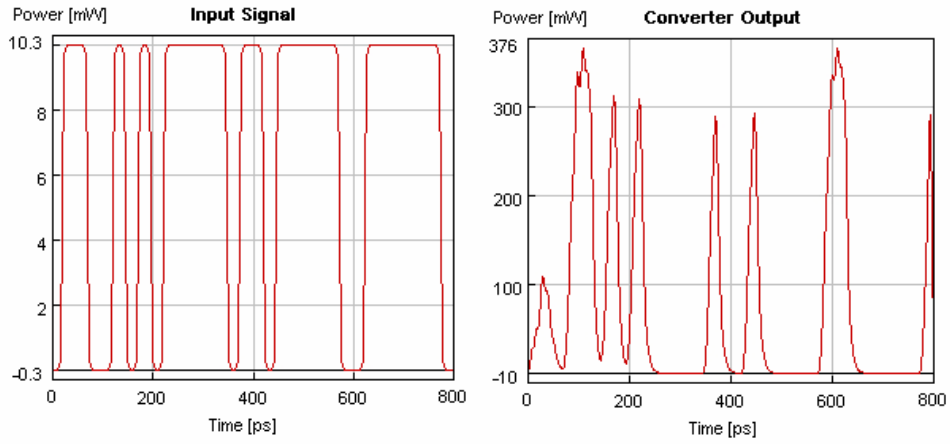

(a) 40 Gbps Input **(b) 40 Gbps Output**

Figure 15: XPM MZI at 40 Gbps

The final topology simulated in this project was an XPM wavelength converter based on a Sagnac interferometer. A Sagnac interferometer, as seen in Figure 16, or in the VPI schematic in Figure 17, is essentially a loop of optical fiber. A nonlinear element, in this case an SOA, has been placed slightly off center in the loop. CW laser light at wavelength λ_2 is split at the loop input by a 3 dB optical coupler, such that half the power travels around the loop in a clockwise fashion and the other half counterclockwise. After propagation around the loop, the power recombines at the coupler and is normally reflected back towards the CW source that it came from if there was no SOA in the loop. Hence, the device is sometimes referred to as a nonlinear optical loop mirror, where the SOA can be used to control the degree to which light is reflected by the mirror. However, when the incoming data signal on wavelength λ_1 is coupled into the loop just before the SOA, the bit pattern of the data signal causes variations in the SOA gain and phase characteristics. Since the SOA is off center in the loop, the clockwise and counterclockwise waves that recombine at the end of the loop traveled through the SOA at different times. Since the SOA imparts different phase and gain characteristics as the data on λ_1 modulates the light, the clockwise and counterclockwise waves experience different gain values and different phase delays. The resulting differences in phase enable some of the optical power to exit the loop on the output port of the coupler, instead of being reflected back towards the CW source. This transmitted power becomes the new signal at λ_2, which is extracted using an optical bandpass filter. Polarization controllers (which also effect the phase of the signals that pass through them) are also included in the loop to control the phasing and alignment of the polarizations of the clockwise and counterclockwise light before they recombine at the end of the loop. The presence of the polarization controllers in the loop makes a dramatic difference in the

output bit pattern, as seen in Figure 18. A more detailed analysis of the Sagnac interferometer based XPM converter is complex, and is outside the scope of this project.

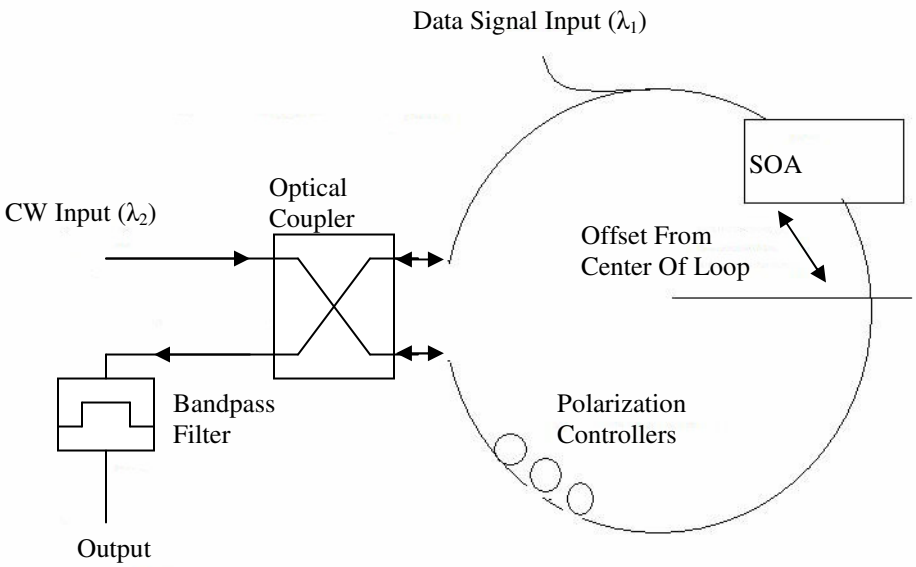

Figure 16: An XPM Sagnac based converter

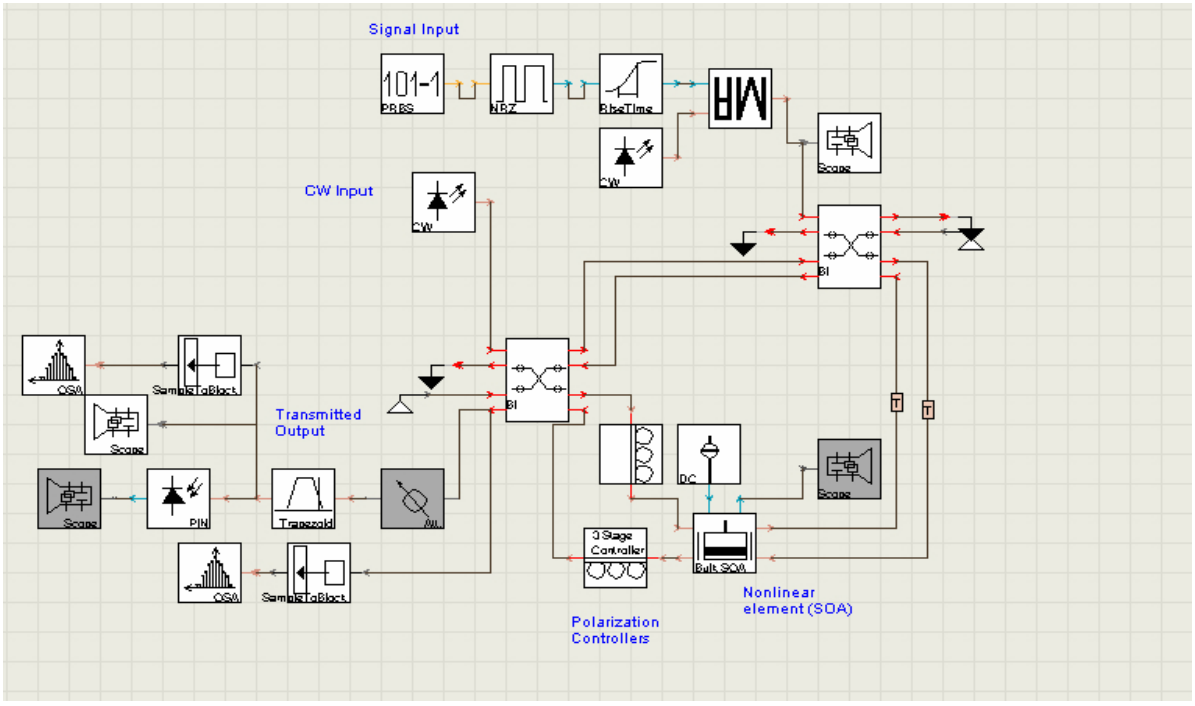

Figure 17: Schematic of an XPM Sagnac based wavelength converter in VPI

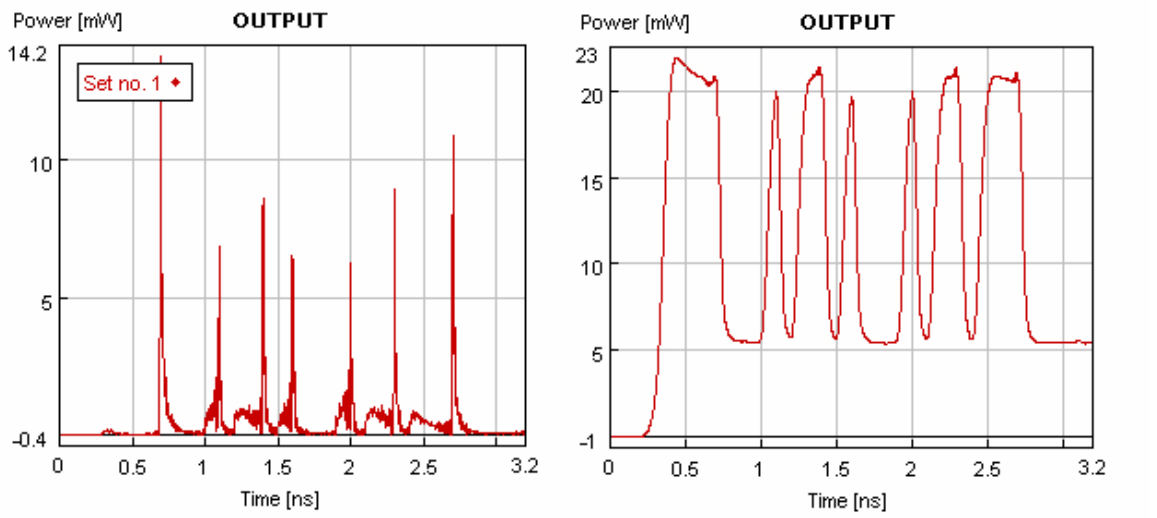

(a) No polarization control **(b) With polarization control**

Figure 18: XPM Sagnac output at 10 Gbps

XGM Construction and Testing

Using the results from the VPI simulations, an XGM type wavelength converter was constructed in hardware. A block diagram of the experimental setup can be seen in Figure 19.

Note the similarities with Figure 8. Distributed feedback (DFB) semiconductor laser diodes were used for the two wavelength sources. The pulse pattern generator was used to imprint a (2^{31} – 1) bit long pseudo-random data stream onto the 1548.51 nm wavelength using a Mach-Zender optical modulator. An Erbium-doped fiber amplifier (EDFA) was used to precisely control the power level of λ_1 that was coupled into the SOA. The WDM multiplexer with an insertion loss of approximately 1.5 dB was used to couple λ_1 and λ_2 into the SOA. An attenuator was used to reduce the output power level to an appropriate value for the optical receiver used. Another WDM device was used as an optical filter at the output of the attenuator to block λ_1. Finally, the resulting signal was viewed on a digital oscilloscope and optical spectrum analyzer, as well as being received by an optical receiver with a receiver sensitivity of -27 dBm. The output of the receiver was used to drive the bit error rate tester (BERT) which counted how many bits received at the end of the link were in error compared to the initial (2^{31} -1) length bit pattern sent by the pulse pattern generator. A variety of drive currents were tried experimentally on the converter. The best results were obtained for drive currents around 350 mA, but conversion was still successful with currents as low as 250 mA and as high as 500 mA.

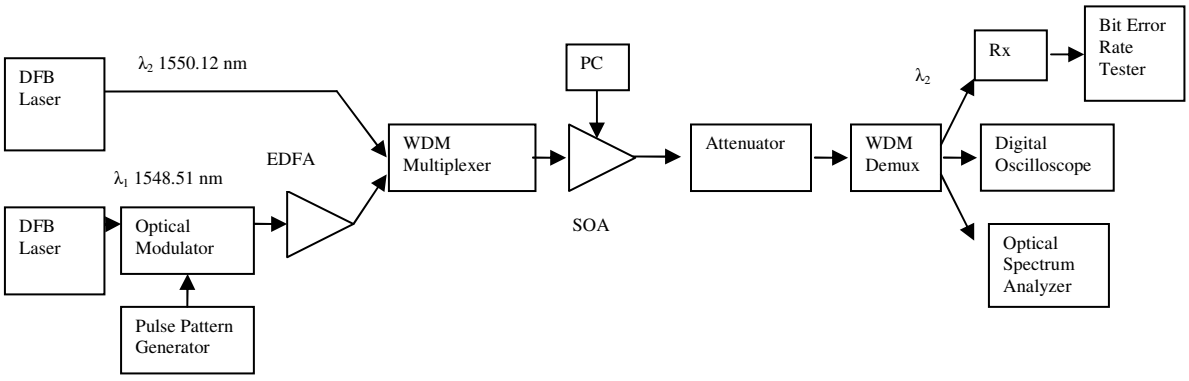

Figure 19: Experimental setup for XGM converter.

With a drive current of 350 mA, wavelength conversion from 1548.51 nm to 1550.12 nm was successfully achieved. The eye diagrams for the input and output of the converter are seen in Figure 20. An eye diagram is basically an oscilloscope trace with the persistence on so that successive bits trace over one another. Therefore, it shows all possible transitions from zero to one and vice versa. An open eye means that the receiver should have little difficulty distinguishing ones from zeros, so the wider the opening at the center of the eye, the better the performance of the link. As the eye closes, however, the signal degrades and the BER increases. The eye diagrams shown in Figure 20 correspond to a 2.5 Gbps bit rate and a 1.61 nm upward conversion in wavelength. The extinction ratio of the input was 12.5 dB, and the extinction ratio of the output was 8 dB, meaning that there was a 4.5 dB degradation as a result of the conversion. The bit error rate (BER) of the output signal in Figure 20 (b) was measured to be better than 10^{-14}, with no errors observed over a 24 hour period. A BER less than 10^{-9} is considered adequate for most fiber optic data networks, so a BER of 10^{-14} is essentially error free performance.

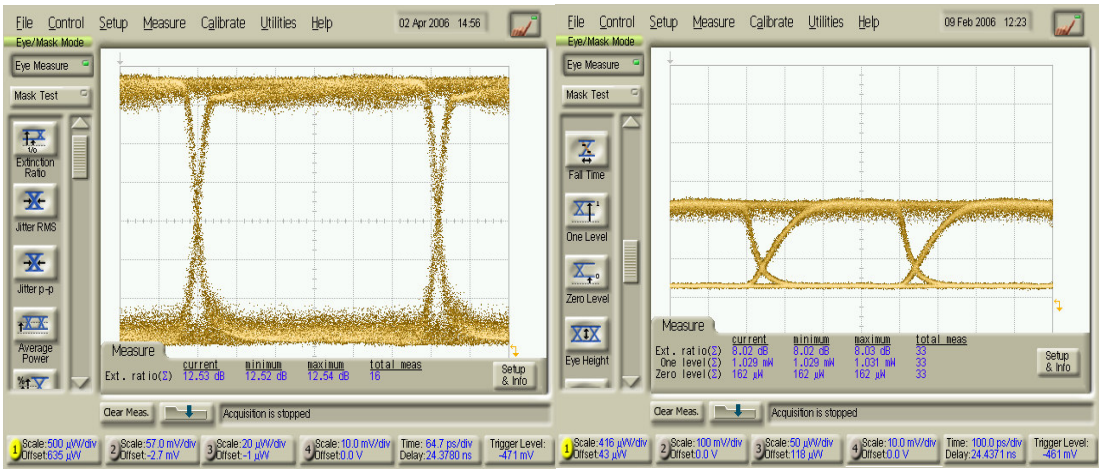

(a) input signal, 1548.51 nm (500µW/div scale) (b) output signal, 1550.12 nm, (416µW/div scale)

Figure 20: XGM wavelength converter at 2.5 Gbps data rate

The conversion range of the XGM converter was determined using a tunable laser as the CW source and a tunable filter on the output of the converter. With an input signal wavelength λ_1 of 1548.51 nm, conversion up or down 13 nm in wavelength was observed with output extinction ratios that varied between 6 dB and 12 dB. The measurement range was limited by the tunable filter, not by the wavelength converter itself. Therefore it is believed that the converter is actually capable of operating over an even wider span of wavelengths. Figure 21 shows the extinction ratio of the output at different converted wavelengths. The output extinction ratio is better for conversions towards shorter wavelengths than for those towards longer wavelengths. This is expected and is due to the differential gain characteristics of the SOA. [4] At the low end of the tunable filter's range, an output extinction ratio of 12 dB is observed, meaning there was less than 0.5 dB of degradation from the input extinction ratio. Conversely, at the extreme upper edge of the filter's range, the output extinction ratio is only about 6 dB, implying a degradation of more than 6 dB in extinction ratio. The impact of the degradation in extinction ratio depends on a number of factors. In these experiments there was minimal impact on the BER because the power levels of the output were so high relative to the noise floor of the receiver used. The receiver used in this project had a sensitivity of -27 dBm, or approximately 2 μW, whereas the power of the light coming out of the converter is on the order of mW. This leads to what is known as a high quality, or Q, factor, implying essentially error free performance, even if the extinction ratio is relatively poor. If there was a significant drop in power level at some point in the optical path then the ratio of received power to the receiver sensitivity would drop significantly, thereby decreasing the Q factor, and increasing BER. This could occur if the fiber lengths were too long or if too many converters were cascaded.

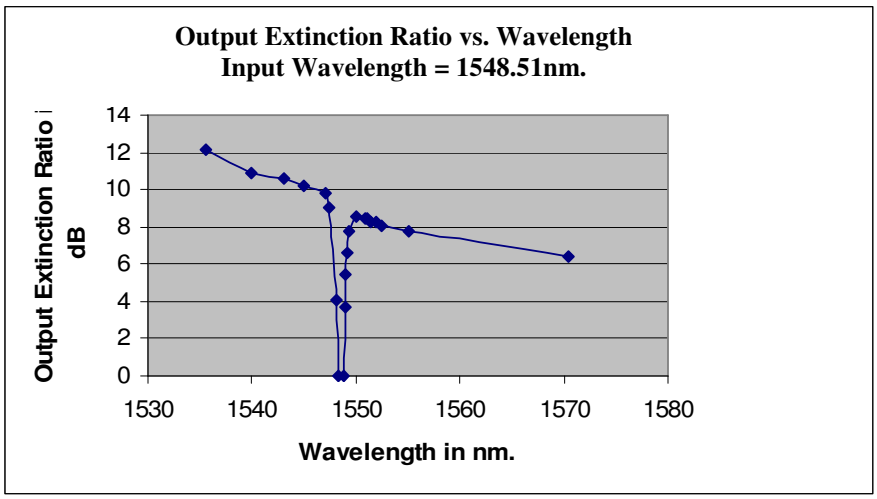

Figure 21: Output extinction ratio vs. converted wavelength

Integration Into LAN

The main thrust of this research was to observe the effects of a wavelength converter in the context of a LAN. As such, an effective method for integrating a wavelength converter into the network was needed. Three main functions are required to use wavelength conversion in the LAN in Figure 2. The first is to direct a signal dropped from the network by the BADM to the receiver located at that node. The second is to add signals from the transmitter at the node to the network using the BADM. Both of these functions can be implemented without wavelength conversion. The last function desired is to drop a signal from the network with the bidirectional add-drop multiplexer (BADM), convert the signal wavelength, and then add the signal back onto the network on the new wavelength. The arrangement shown in Figure 22 supports all three of these functions as illustrated for Node 4 of the LAN in Figure 2. At the first set of switches, represented by the two purple blocks on the left, information dropped by the BADM can either be sent to a receiver if Node 4 is the end destination of the data, or it can be sent into the wavelength conversion stage where it can be converted to one of the two outgoing wavelengths. The set of switches on the right controls which signals are added back onto the network. The user

has the choice of adding information back onto the network either from the transmitter at Node 4 or from the output of a wavelength converter.

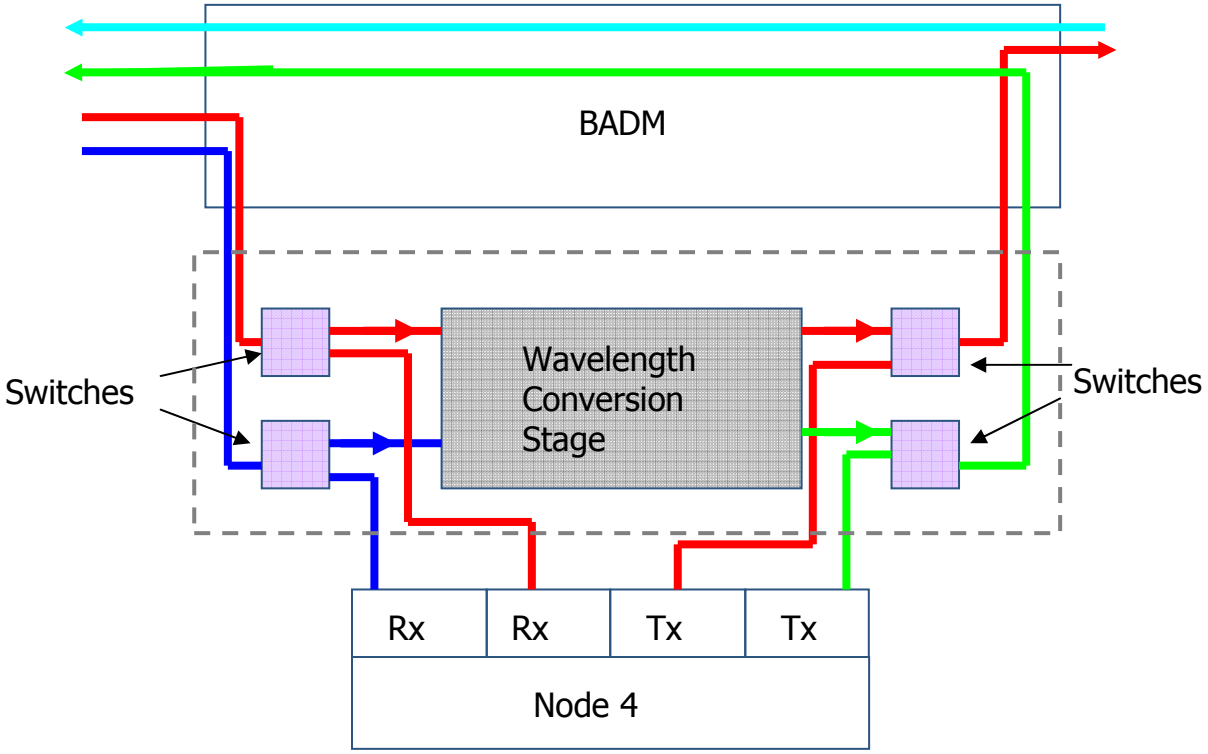

Figure 22: Integration of wavelength conversion at a node

Figure 23 shows a more detailed configuration of the components in the dashed box of Figure 22. The four switches from Figure 22 are also shown as a reference. Signals propagate through Figure 23 from left to right. After a signal enters the wavelength conversion stage, a 1x2 switch directs the signal to the proper wavelength converter, labeled as WC. The signal is then used as the input to one of the wavelength converters. At the output of the converter, the signal passes through another switch meant to prevent two signals from trying to convert to the same wavelength at once. Finally, the signal, on the new wavelength, passes through the last switch on the right and is added to the network by the BADM. The mechanism used to control the switch states is an important issue that must be examined in further research.

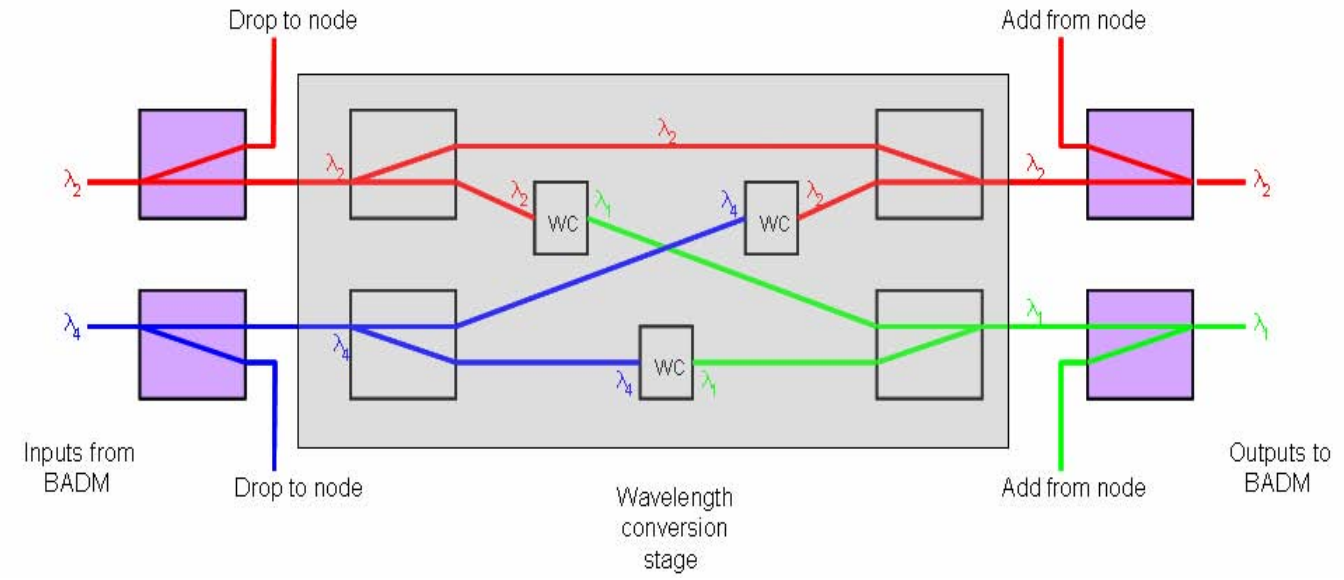

Figure 23: Schematic of the wavelength conversion stage of Node 4

The schematics shown in Figures 22 and 23 were used to integrate two XGM converters into the network as a proof of principle, accounting for all possible losses in the node. The switches were set to convert the incoming red wavelength (1550.12 nm) to the green wavelength (1550.92 nm) and the incoming blue wavelength (1548.51 nm) to the red wavelength (1550.12 nm). A simplified representation of the experimental setup can be seen in Figure 24. As an example, a digital data stream on the blue wavelength (that was launched from Node 5 in Figure 2) is dropped at Node 4 by the BADM and is converted to the red wavelength. The converted signal on the red wavelength is added back to the network and is eventually dropped at Node 3. Figure 25 shows the eye diagram of the converted signal after it is dropped from the network at Node 3. The extinction ratio is 7 dB, roughly 1 dB worse than when conversion is achieved between the same two wavelengths without the network present.

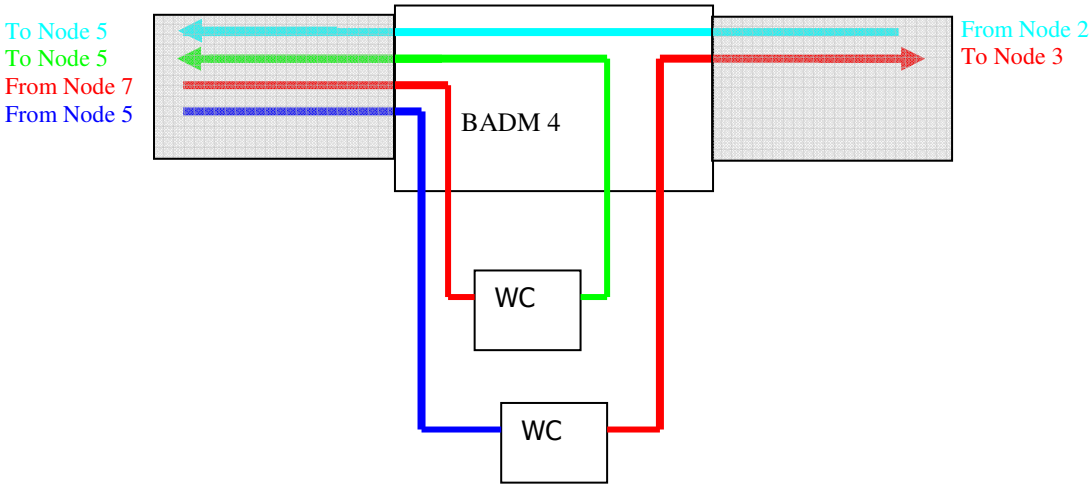

Figure 24: Signal paths at Node 4

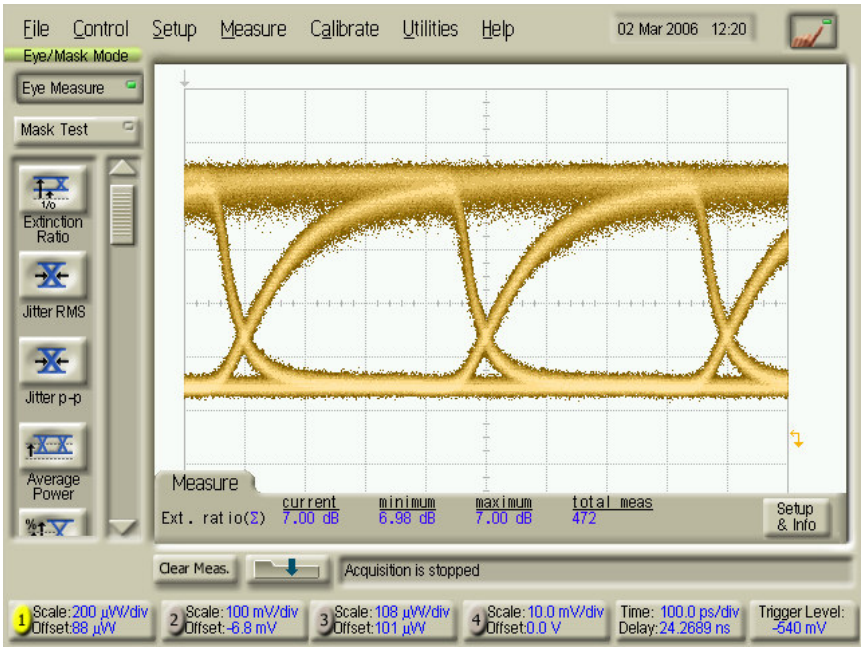

Figure 25: Eye diagram of converted signal at Node 3

Having demonstrated conversion at a single node, a network path that required cascaded conversion was selected. For an eight node ShuffleNet, two conversions would be required for maximum of three hops needed between any two nodes (see Figure 1). Figure 26 depicts the path that was tested. Data is transmitted from Node 5 on the blue (1548.51 nm) wavelength, converted

to the red (1550.12 nm) wavelength at Node 4, and then converted back to the blue wavelength at Node 3. The signal is dropped from the network at Node 2 after undergoing two wavelength conversions (three hops). Unfortunately, no amplifier (EDFA) was available for use in the second wavelength converter. While the BER in the received signal was still better than 10^{-14}, the extinction ratio was only 2.88 dB, as seen in Figure 27. If there were more nodes in the network, resulting in additional hops and additional conversions, the BER would assuredly increase. Hence, an EDFA is required in the second converter before any conclusions can be made regarding cascadability in this network.

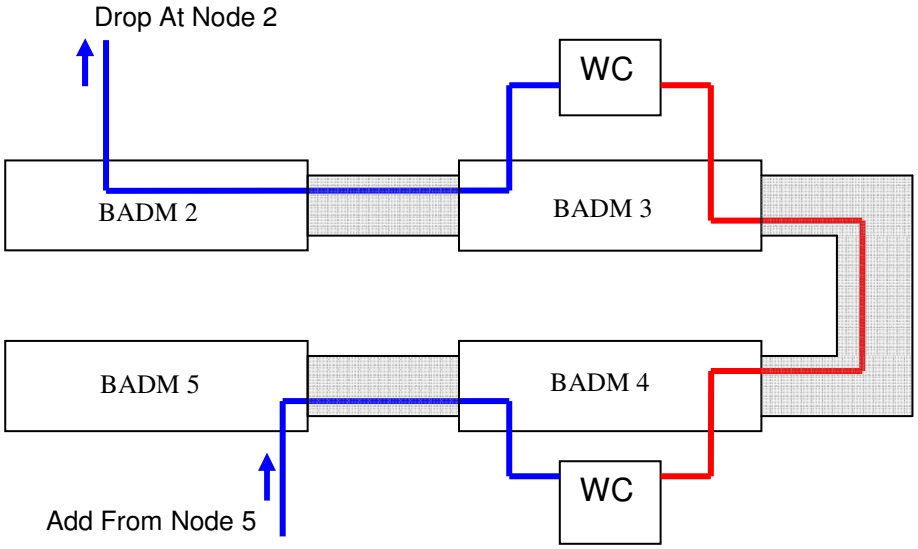

Figure 26: Network path using cascaded wavelength converters

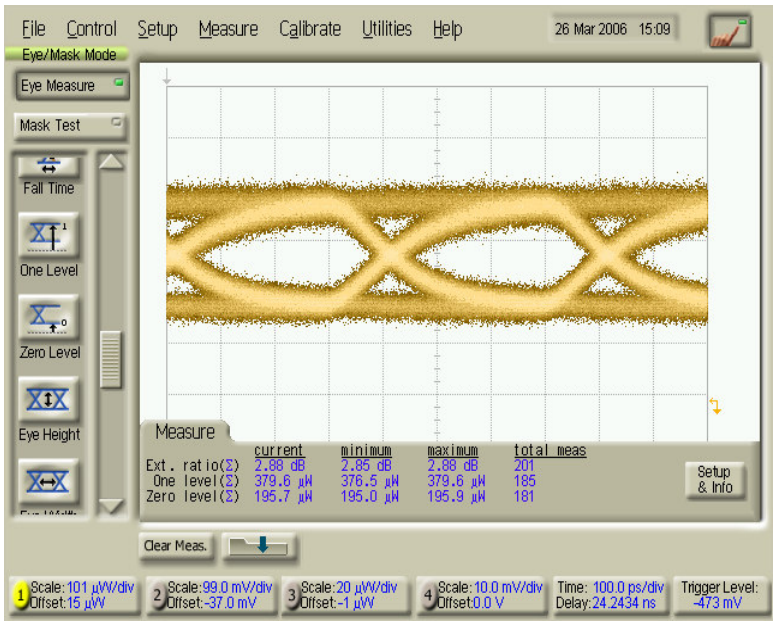

Figure 27: Eye pattern of received signal after cascaded conversions in the network

Latency

A primary reason to integrate wavelength conversion into a network is to increase throughput by reducing latency, the time it takes to physically transmit a sequence of bits through the network. Using the O-E-O conversion method, last year Joshua Wort was able to design a network interface card (NIC) in his Trident project that demonstrated an end to end latency of approximately 314 ns. [8] For comparison, latency measurements were taken on each component that made up the XGM converter, and on the conversion stage of a node as a whole. The test configuration can be seen in Figure 28. The overall latency from the input of the first switch in Figure 28 to the output of the last switch was measured to be approximately 235 ns. This measurement was taken by observing the time at which a particular sequence of bits from a $(2^{11} - 1)$ length bit pattern appeared at the input to the first switch and the time at which the inverted version of that bit pattern arrived at the end of the last switch on the new wavelength using two input channels on a digital oscilloscope. The test was repeated for a $(2^{15} - 1)$ length bit

pattern to ensure that the bit pattern was not wrapping around on itself. Latency measurements for each component in the converter can be seen in Table 2. The most significant source of latency was the EDFA which was used to boost the power level of the input signal. The latency from the WDM demultiplexer can be subtracted since the device is not needed in the node in Figure 23. Hence, the entire node latency of approximately 209 ns is a 33% reduction in latency from Wort's results. The latency measured here could be reduced signifigantly by eliminating jumper cables and integrating the components in a more efficient manner. This would likely reduce the latency by another 40 or 50 ns.

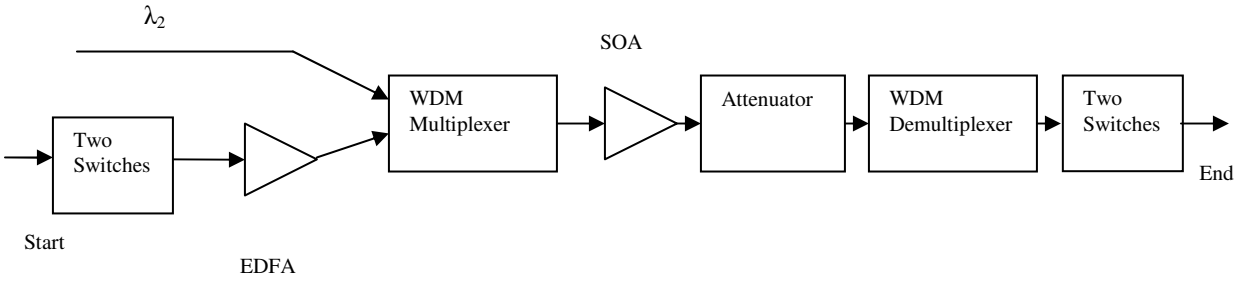

Figure 28: Experimental setup for latency measurement

Component	Measured Latency (ns)
Each Switch	10.3
EDFA	56
Each MUX/DEMUX	26
SOA	11.4
Attenuator	33

Table 2: Latency measurements for converter components

Mixed Signal Analysis

Since it is ultimately desired that the network support transmission of both analog and digital data, various measurements were made on the LAN to determine the feasibility of routing analog and digital signals simultaneously. For digital signals passing through the network, the output eye diagram was examined to determine how much degradation the signal had

experienced. For analog radio frequency (RF) signals spur free dynamic range (SFDR) was measured using a two tone test.

SFDR is a measure of the maximum usable signal to noise ratio (SNR) that can be achieved in a link before nonlinear harmonic distortion, observed as spurs in the RF spectrum, begins to degrade the signal. To measure SFDR on an optical link, two RF tones at frequencies f_1 and f_2 are transmitted on a single wavelength channel. The difference in the RF frequencies, $f_2 - f_1$, is relatively small, as seen in Figure 29, where two tones at 999 MHz and 1000 MHz are transmitted. As the power in these tones increases, nonlinear third order spurs begin to develop and grow at frequencies of $2f_2 - f_1$ and $2f_1 - f_2$. Such spurs typically develop because of nonlinearity in the optical modulator transfer function. The power in each spur rises as a function of P_{in}^3, causing distortion in the original signal at higher power levels. Hence there is a balance between increasing the power to improve SNR and avoiding distortion. The SFDR defines the optimal operating point where SNR is maximized without causing distortion.

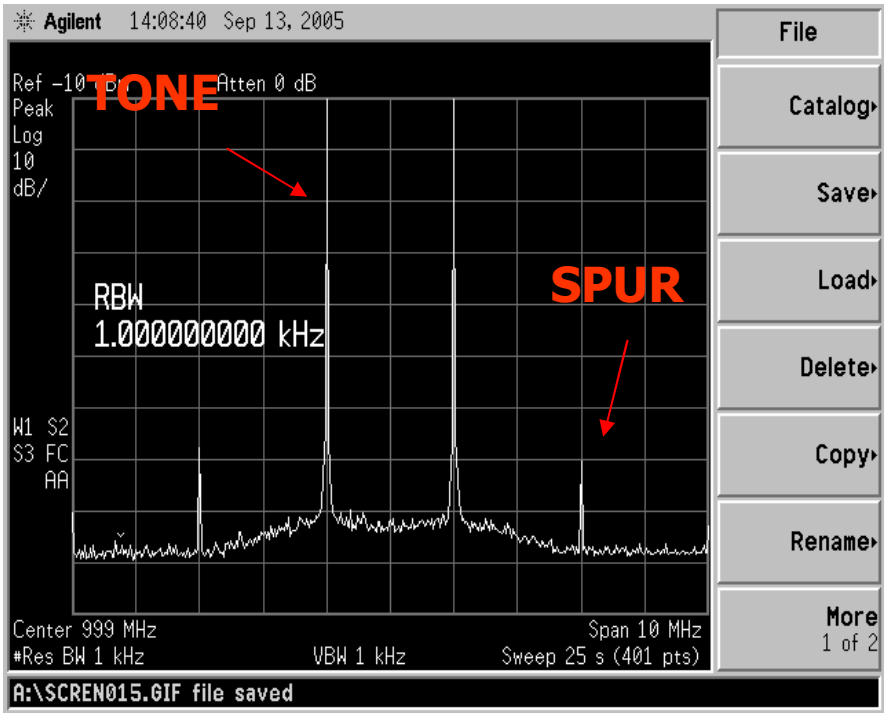

Figure 29: RF spectrum depicting two tone test for spur free dynamic range

SFDR is computed using a plot of the power levels of the fundamental tones and the third order spurs as the input power is increased, as seen in Figure 30 for the fundamental tone at 1 GHz. The x and o symbols correspond to measured data points. The point at which the best fit lines for the data intercept is defined as the third order output intercept point (OIP3).At this point, the power in the spurs would, in theory, be equal to the power in the fundamental tones if the power in the RF tones were increased sufficiently. In reality, this power level is hard to achieve, and as such, extrapolation is necessary. The noise floor of the system is then measured. Since the spur power in dBm (decibels in reference to 1 mW instead of 1W) increases at a rate three times that of the fundamental, the SFDR is two-thirds of the difference between OIP3 and the noise floor.

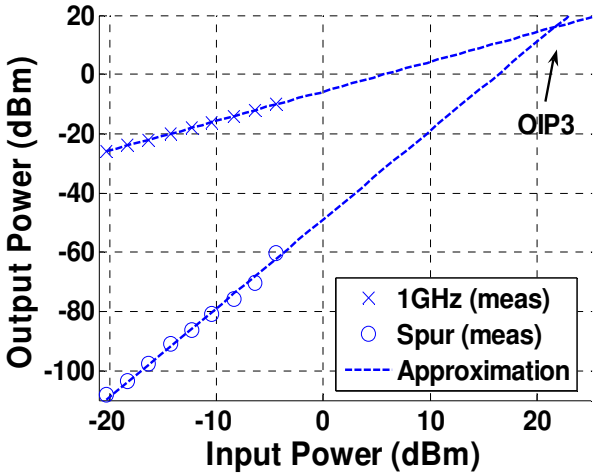

Figure 30: Finding SFDR from the tone power and spur power

Figure 31 shows a block diagram of the experimental configuration that uses four signals (two analog and two digital) propagating through the network on four different wavelength channels, where the BADMs in the ring are labeled a-h. Using this setup we measured an SFDR of 113 dB-Hz$^{2/3}$. The required value of SFDR is application specific, but values above 100 dB-Hz$^{2/3}$ are generally acceptable. We also received a clear, open eye pattern on the 10 Gbps digital data channel, as seen in Figure 32. The complete optical spectrum, measured just after the amplifier in Figure 31, can be seen in Figure 33.

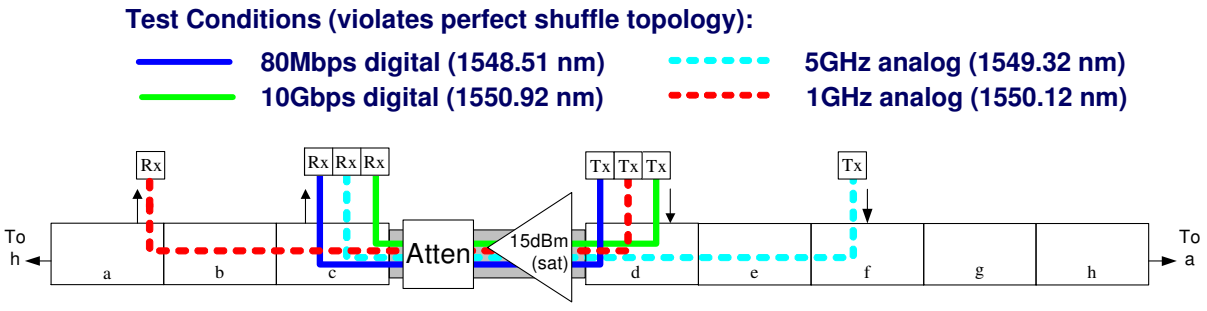

Figure 31: Test conditions for mixed signal analysis

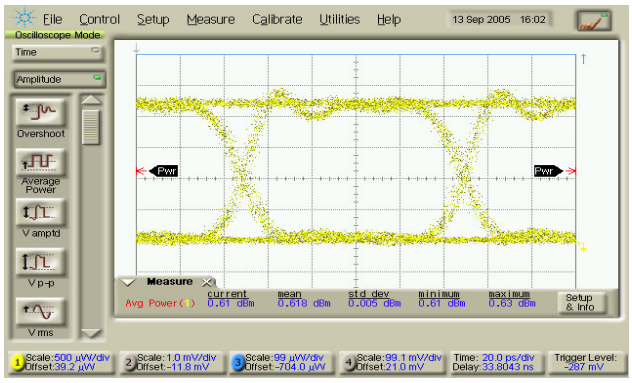

Figure 32: 10 Gbps digital channel in mixed signal environment

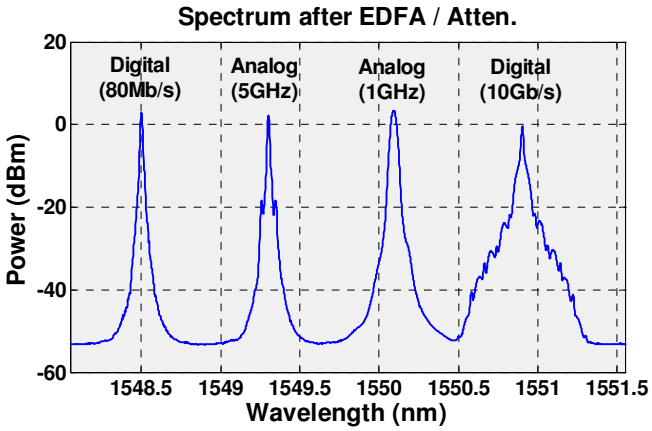

Figure 33: Mixed signal network optical spectrum

After determining the baseline mixed signal performance levels for the network, analog wavelength conversion was attempted. A 15 MHz sine wave on a 1548.51 nm carrier was used as the input to an XGM converter. The output wavelength of the converter was 1550.12 nm. The input signal can be seen in Figure 34 (a) and the converter output can be seen in Figure 34 (b). There was significant degradation evident in the output signal. Due to time constraints, little effort was made to optimize the analog conversion process and chances for success are low given results published in literature [5]. In its current state, the XGM converter is not suitable for analog signals, and no comparison to the baseline SFDR measurements can be made yet.

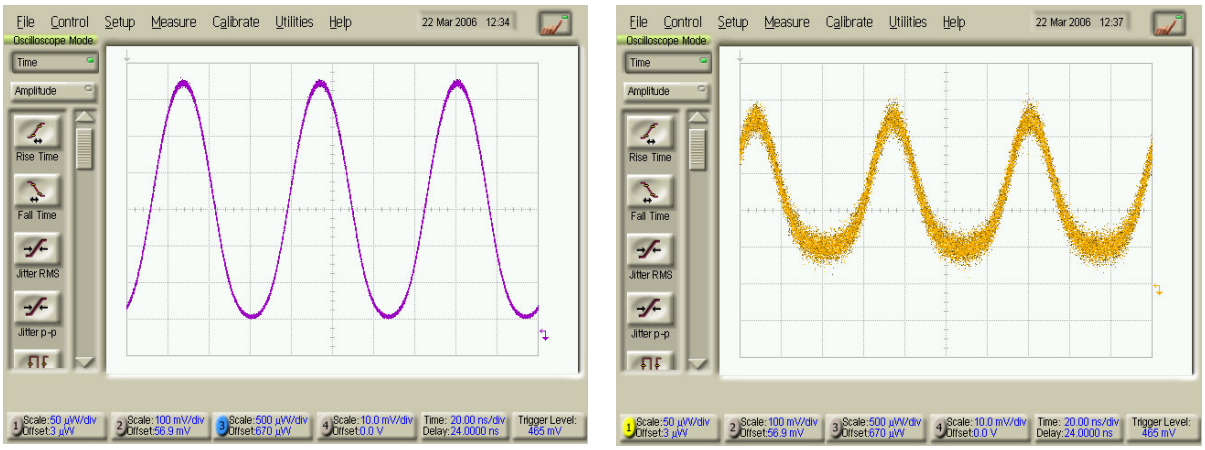

(a) input, 15 MHz sine wave, 1548.51 nm **(b) converter output, 1550.12 nm**

Figure 34: Effects of XGM converter on analog signal

Conclusion

This project successfully demonstrated the feasibility of using all-optical wavelength conversion in a LAN. Error free digital performance for both single and cascaded conversion was observed for an XGM converter implemented in hardware over a twenty-four hour period. The plot in Figure 21 confirms previously published results predicting degradation in the extinction ratio of an XGM wavelength converter. Simulation results suggest operation up to 10 Gbps should be possible with XGM converters and operation up to 20 Gbps should be possible with an XPM type converter.

A model for integrating wavelength converters into the network nodes in Figure 2 was developed. This allowed data dropped by a BADM at a node to either be routed to a receiver or to be converted to a new wavelength and added back to the network. With cascaded wavelength converters in the network, for a maximum of three hops in Figure 1, error free performance was observed. There was also greater than a 30% reduction in latency over experimental results for the O-E-O conversion method obtained in [8], with a total latency of 209 ns through the

wavelength conversion stage of Figure 23. Furthermore, the plot seen in Figure 21 confirms results previously published in literature about XGM converter extinction ratios.

Wavelength conversion for analog signals was not successful in this project. However, more time is needed to study analog conversion before it can be definitively determined whether it is possible. However, the baseline mixed signal measurements taken on the network give us a solid base with which to compare any future results. Although no comparisons to baseline measurements can be made yet for analog conversion, the collection of the SFDR data further extended our knowledge of the network's capabilities.

To truly demonstrate the potential of all-optical wavelength conversion in a LAN, an effective algorithm must be developed to set the state of the switches in Figure 23. Reduction in latency and the capability for low BER performance have already been established. If an effective method of controlling the routing decision is found, all-optical wavelength conversion promises to significantly enhance performance in fiber optic networks.

Bibliography

[1] Maier, Martin and Reisslein, Martin. "AWG-Based Metro WDM Networking." *IEEE Optical Communications*. November 2004.

[2] Fisher, Adam. "A Wavelength Multiplexed Bidirectional Fiber Ring Network". USNA Trident Project Final Report, 2004.

[3] Wolfson, D., Fjelde, T., and Kloch, A.. "Technologies for All-Optical Wavelength Conversion in DWDM Networks." *Lasers and Electro-optics*. Vol. 2, July 2001.

[4] Durhuus, Terji, et al. "All-Optical Wavelength Conversion by Semiconductor Optical Amplifiers." *Journal of Lightwave Technology*. Vol. 14 June 1996.

[5] Yoo, S. J. B. "Wavelength Conversion Technologies for WDM Network Applications." *Journal of Lightwave Technology.* Vol. 14, June 1996.

[6] Eiselt, M., Pieper, W., and Weber, H. G. "SLALOM: Semiconductor Laser Amplifier in a Loop Mirror." *Journal of Lightwave Technology.* Vol. 13, November 1995

[7] Keisser, Gerd. Optical Fiber Communications, Third Edition. Boston, MA: McGraw Hill, 2000.

[8] Wort, Joshua. "A Network Interface Card for a Bidirectional Wavelength Division Multiplexed Fiber Optic Local Area Network." USNA Trident Project. Final Report, 2005.

Appendix A: Glossary of Terms

BER: Bit Error Rate, a ratio of the total number of bits received in error to the total number of bits transmitted. For modern telecommunications and data networks, a BER of 10^{-9} or better is standard.
CW: Continuous Wave, laser light that is not modulated by data.
DFG: Difference Frequency Generation, a wavelength conversion technique that uses a nonlinear medium to transfer data from an incident wavelength to a different wavelength without producing the unnecessary satellite wavelength found in FWM converters.
DWDM: Dense Wavelength Division Multiplexing, WDM with the frequencies (or wavelengths) located closer together in the spectrum.
EDFA: Erbium-Doped Fiber Amplifier, an optical amplifier that is based on implanting small amounts of Erbium into a silica fiber.
FWM: Four-Wave Mixing, a wavelength conversion technique that relies on the interaction of a data signal and a CW probe signal in a nonlinear medium to transfer data from the incident wavelength to a different wavelength.
Gbps: Gigabit per second, a unit of measure that describes how many bits per second a link is capable of handling.
LAN: Local Area Network, a computer network that often does not exceed the size of a building
O-E-O conversion: Optical-Electrical-Optical conversion, the process by which information is taken from an optical format to an electrical format so that a node's routing circuitry can make a routing decision and made back into an optical signal for retransmission onto the network.
Rx: Receiver.
SOA: Semiconductor Optical Amplifier, an optical amplifier commonly used in XGM and XPM converters.
SFDR: Spur-Free Dynamic Range, a measurement that describes the best possible analog signal-to-noise ratio that an optical link can achieve. SFDR Is an important performance metric for analog and mixed signal networks.
Tx: Transmitter.
VPI Photonics: A computer simulation software package used to help simulate optical devices and links.
WDM: Wavelength Division Multiplexing, a method to increase utilization of a fiber's bandwidth by sending multiple frequencies of light down one fiber optical cable.
XGM: Cross-Gain Modulation, a wavelength conversion technique that utilizes the gain saturation characteristics of a semiconductor optical amplifier (SOA) to imprint data from one wavelength to another.
XPM: Cross-Phase Modulation, a wavelength conversion technique that utilizes both the gain and phase dynamics of SOAs and some sort of interferometer to imprint data from one wavelength to another.